QUANTITATIVE EPMA COMPOSITIONAL MAPPING OF NWA 2995: CHARACTERIZATION AND PETROLOGIC INTERPRETATION OF MAFIC CLASTS. P. K. Carpenter[1], T.M. Hahn[1], R.L. Korotev[1], R.A. Zeigler[2], B. L. Jolliff[1], [1]Dept. Earth and Planetary Sciences and the McDonnell Center for the Space Sciences, Washington University in St. Louis, Campus Box 1169, Saint Louis, MO, 63130 (paulc@levee.wustl.edu) , [2]NASA Johnson Space Center, Mail Code X12, Houston, TX, 77058.

Introduction: We present the first fully quantitative compositional maps of lunar meteorite NWA 2995 using electron microprobe stage mapping, and compare selected clast mineralogy and chemistry. NWA 2995 is a feldspathic fragmental breccia containing numerous highland fine grained lithologies, including anorthosite, norite, olivine basalt, subophitic basalt, gabbro, KREEP-like basalt, granulitic and glassy impact melts, coarse-grained mineral fragments, Fe-Ni metal, and glassy matrix [1]. Chips of NWA 2995, representing these diverse materials, were analyzed by INAA and fused-bead electron-probe microanalysis (EPMA); comparison of analytical data suggests grouping of lunar meteorites NWA 2995, 2996, 3190, 4503, 5151, and 5152. The mean composition of NWA 2995 corresponds to a 2:1 mixture of feldspathic and mare material, with approximately 5% KREEP component [2]. Clast mineral chemistry and petrologic interpretation of paired stone NWA 2996 has been reported by Mercer et al. [3], and Gross et al. [4]. This study combines advances in quantitative EPMA compositional mapping and data analysis, as applied to selected mafic clasts in a polished section of NWA 2995, to investigate the origin of mafic lithic components and to demonstrate a procedural framework for petrologic analysis.

Quantitative EPMA compositional mapping: We continue development of quantitative compositional mapping as outlined previously [5], using the JEOL JXA-8200 electron microprobe at Washington University, with JEOL and Probe Software operating systems to acquire backscattered-electron (BSE) and X-ray map data, and point analyses for major- and trace-element concentrations. Stage translation with a fixed electron beam is used with energy-dispersive (EDS) and wavelength-dispersive spectrometers (WDS) to obtain X-ray intensity maps. The WDS maps are converted to concentration maps using the CalcImage program, which performs a full $\Phi(\rho z)$ matrix correction according to C = k * ZAF, where C is the concentration, k is the background-corrected X-ray intensity emitted from the sample relative to a calibration standard, and individual factors Z, A, and F correct for matrix effects. The WDS background correction uses the mean atomic number (MAN) background correction method from a suite of EPMA standards and establishes an analysis-specific background for all WDS elements as part of the ZAF correction. EPMA stage mapping is performed at relatively high probe current to compensate for reduced pixel dwell time, and coupled with background correction using the MAN calibrations, all mapping time is spent at the WDS X-ray peak positions.

The resulting maps contain a complete element wt.% analysis at each pixel, and additional maps are generated for background intensity, mineral formulae, and element detection limits. These maps are further analyzed using a procedure that includes visualization and processing using Golden Software Surfer, Matlab, and ENVI.

Compositional analysis of NWA 2995: A "slab" of NWA 2995 approximately 19×11 mm and 4 mm thick was prepared for EPMA analysis. A high resolution mosaic BSE image was used for subsequent selection of stage map areas. Maps were acquired at 15 kV, 100 nA probe current, and dwell times of 25-50 msec at 1024×1024 pixel resolution and stage step size of 2-7 μm per pixel, with run times of 16-24 hours. Two large maps effectively sample the entire section (Maps 1 and 2), and smaller maps were then centered on selected mafic clasts (B, G, and H) as outlined in Fig. 1.

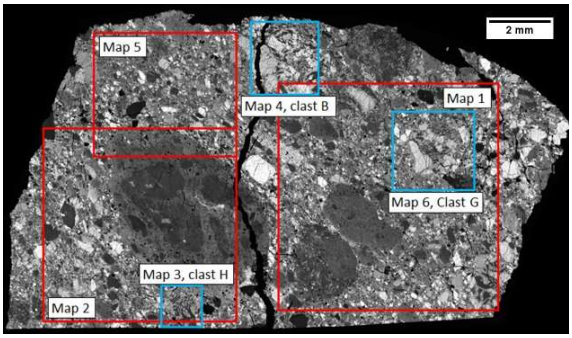

Figure 1. BSE mosaic locator for NWA 2995. Map areas 1 and 2 outlined in red, clast map areas outlined in blue.

Data were collected in two passes of 5 WDS elements each, to obtain a 10 element analysis at each pixel, and the maps were processed as outlined above. The resulting data set consists of 1024^2 fully quantitative analyses per map. These analyses were processed and classified by assignment to mineral phase categories, and corrected to remove data acquired on cracks and epoxy. The classification procedure results in unique assignment of each pixel to a mineral phase, and the summation of all pixels in each phase was used to calculate the modal abundance of olivine, low- and

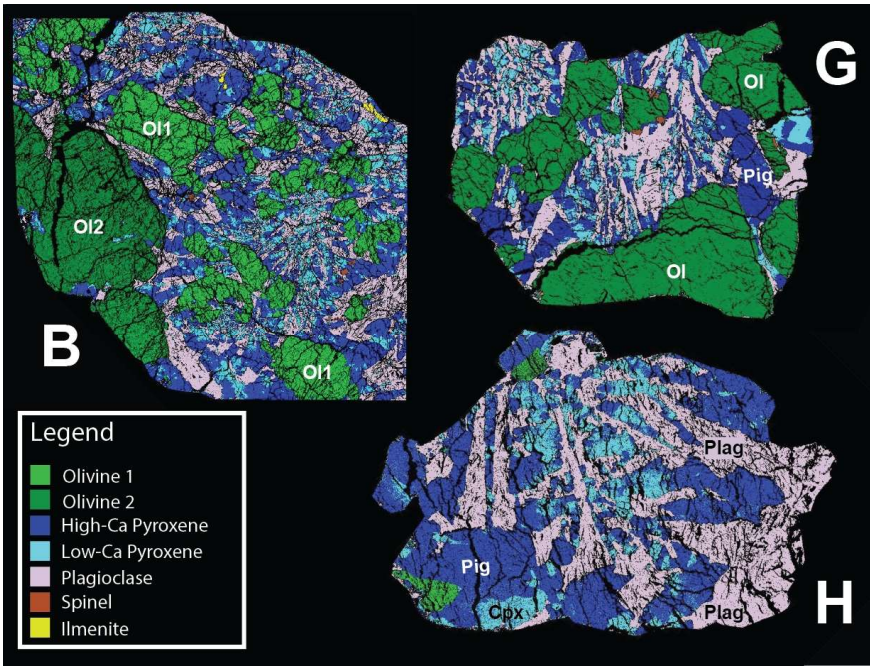

Figure 2. Classification images of mafic clasts in NWA 2995. Clast width: B (2150 μm), G (1360 μm), and H (1200 μm).

Table 1. Compositional data for NWA 2995

Oxide	Clast B	Clast G	Clast H	Maps 1 & 2	Matrix	Fused Bead
SiO_2	43.4	43.6	49.6	45.7	46.3	46.20
TiO_2	0.42	0.22	0.29	0.45	0.53	0.68
Al_2O_3	7.44	6.96	15.2	19.9	21.4	20.60
Cr_2O_3	0.31	0.34	0.38	0.20	0.20	0.23
FeO	21.0	19.8	10.0	10.5	9.65	9.75
MnO	0.27	0.26	0.19	0.15	0.13	0.15
MgO	19.8	22.3	12.8	9.73	8.11	8.08
CaO	7.24	6.53	12.8	12.6s	13.1	13.50
Na_2O	0.22	0.22	0.44	0.55	0.60	0.51
K_2O	0.02	0.03	0.05	0.12	0.15	0.19
Total	100.1	100.2	101.7	99.8	100.2	99.89
Mg#	62.7	66.7	69.5	62.2	60.0	59.6

Phase	Clast B	Clast G	Clast H	Clast B	Clast G	Clast H
High-Ca Px	11.0	10.2	15.8	Wo33-En45-Fs22	Wo35-En48-Fs17	Wo33-En49-Fs18
Low-Ca Px	25.1	20.7	38.2	Wo14-En54-Fs32	Wo13-En60-Fs26	Wo13-En60-Fs27
Plagioclase	22.8	21.3	44.4	An91-Ab9-Or0.6	An89-Ab10-Or0.7	An90-Ab9-Or0.6
Olivine	22.7	47.6	1.68	Fo58-Fa42	Fo65-Fa35	Fo66-Fa34
Olivine 2	18.0			Fo68-Fa32		
Ilmenite	0.20					
Spinel	0.36	0.27				

high-Ca pyroxene, plagioclase, ilmenite, and spinel. Element concentration data were further used to calculate an average mineral analysis using all pixels assigned to a given phase (lower part of Table 1). Finally, a density-corrected bulk composition was calculated for each mafic clast using the measured modal abundance, elemental composition, and an appropriate phase density (upper part of Table 1). Depending on modal abundance, each phase represents from 10^3 – 10^5 quantitative analyses.

Discussion: Mineral classification maps for mafic clasts B, G, and H are shown in Fig. 2. All quantitative EPMA compositional data are detailed in Table 1, where the density-corrected bulk composition of each clast is compared with: (a) the bulk data for NWA 2995 (Maps 1 and 2), which represents a large area of the slab; (b) the matrix data, which is representative of the slab with clasts subtracted; and (c), with the EPMA fused-bead analysis of [2]. Clasts B and G are subophitic olivine basalts (possibly too small to be representative, and containing excess olivine), and clast H is an ophitic olivine gabbro. Clast B contains subhedral olivine of two distinct compositions, low- and high-Ca pyroxene, ilmenite, and spinel, and has a basaltic composition with comparatively high-Fe content. Clast G contains olivine, low-Ca pyroxene, plagioclase, and spinel. Clast H contains low- and high-Ca pyroxene, plagioclase, minor olivine, and has a relatively aluminous composition.

There is excellent agreement between the matrix data determined by compositional mapping and the fused-bead EPMA data acquired previously, indicating that both techniques can be used to accurately measure the bulk composition of meteorites as represented by subsampled areas. A main advantage of quantitative EPMA compositional map data is in comparison of areas representing spatial domains of essentially point analyses, phases, and lithic regions. This advantage can be used to compare clast and matrix composition, characterize mineral zoning, and to determine the abundance of mineral fragments and glass, for example. In addition to treatment of map data using fully quantified concentrations, the procedure outlined here can be used to characterize samples based on the classification definitions developed on an initial set of maps, rather than requiring intensive inspection of each new map.

Acknowledgement: We thank Jim Strope for donation of the NWA 2995 sample.

References: [1] Bunch et al. (2006) *69th Annual METSOC*, #5254. [2] Korotev et al. (2006) *MAPS* 44, 9, 1287-1322. [3] Mercer et al. (2013) *MAPS* 48, 2, 289-315. [4] Gross et al. (2014) *EPSL* 388, 318-328. [5] Carpenter et al. (2013) *LPSC 44th* #1827